Absolutely Calibrated Vacuum Ultraviolet Spectra in the 150 nm to 250 nm Range from Plasmas Generated by the NIKE KrF Laser

J. F. Seely

Space Science Division, Naval Research Laboratory, Washington DC 20375

Uri Feldman

ARTEP Inc., Ellicott City MD 21042

G. E. Holland

SFA Inc., 9315 Largo Drive, West Suite 200, Largo MD 20774

J. L. Weaver, A. N. Mostovych, S. P. Obenschain, A. J. Schmitt, and R. Lehmberg

Plasma Physics Division, Naval Research Laboratory, Washington DC 20375

Benjawan Kjornarattanawanich

National Synchrotron Light Sources, Brookhaven National Laboratory, Upton NY 11973

and Universities Space Research Associates, Columbia MD 21044

C. A. Back

Lawrence Livermore National Laboratory, Livermore CA 94550

Report Documentation Page

Form Approved
OMB No. 0704-0188

1. REPORT DATE	2. REPORT TYPE	3. DATES COVERED
2005		**00-00-2005 to 00-00-2005**

4. TITLE AND SUBTITLE	5a. CONTRACT NUMBER
Absolutely Calibrated Vacuum Ultraviolet Spectra in the 150 nm to 250 nm Range from Plasmas Generated by the NIKE KrF Laser	5b. GRANT NUMBER
	5c. PROGRAM ELEMENT NUMBER
6. AUTHOR(S)	5d. PROJECT NUMBER
	5e. TASK NUMBER
	5f. WORK UNIT NUMBER
7. PERFORMING ORGANIZATION NAME(S) AND ADDRESS(ES) **Naval Research Laboratory,Plasma Physics Division,4555 Overlook Avenue SW,Washington,DC,20375**	8. PERFORMING ORGANIZATION REPORT NUMBER
9. SPONSORING/MONITORING AGENCY NAME(S) AND ADDRESS(ES)	10. SPONSOR/MONITOR'S ACRONYM(S)
	11. SPONSOR/MONITOR'S REPORT NUMBER(S)

12. DISTRIBUTION/AVAILABILITY STATEMENT
Approved for public release; distribution unlimited

13. SUPPLEMENTARY NOTES
This article appears in the Physics of Plasmas and can be found at Seely et al., Physics of Plasmas 12, 062701 (2005)

14. ABSTRACT

High resolution vacuum ultraviolet (VUV) spectra were recorded from plasmas generated by the NIKE KrF laser for the purpose of observing emission from the two-plasmon decay instability (TPDI) at 2/3 the NIKE wavelength (165 nm). The targets were irradiated by up to 43 overlapping beams with intensity up to ≈1014 W/cm2 and with beam smoothing by induced spatial incoherence (ISI). The targets consisted of planar foils of CH, BN, Al, Si, S, Ti, Pd, and Au. Titanium-doped silica aerogels in pyrex cylinders were also irradiated. Spectra of the target elements were observed from charge states ranging from the neutral atoms to 5 times ionized. The spectrometer was absolutely calibrated using synchrotron radiation, and absolute VUV plasma emission intensities were determined. Emission from the TPDI at 165 nm wavelength was not observed from any of the irradiated targets. An upper bound on the possible TPDI emission was less than 4x10-8 the incident NIKE laser energy. The NIKE laser radiation backscattered from the silica aerogel targets at 248 nm was typically 6x10-6 the incident NIKE laser energy, and the spectral broadening corresponded to the 1 THz bandwidth of the ISI smoothing. The spectra from the moderately charged plasma ions (up to 5 times ionized), spectral line widths, absolute continuum emission level, and slope of the continuum were consistent with plasma temperatures in the 100 eV to 300 eV range.

15. SUBJECT TERMS

16. SECURITY CLASSIFICATION OF:			17. LIMITATION OF ABSTRACT	18. NUMBER OF PAGES	19a. NAME OF RESPONSIBLE PERSON
a. REPORT **unclassified**	b. ABSTRACT **unclassified**	c. THIS PAGE **unclassified**	**Same as Report (SAR)**	**30**	

Abstract

High resolution vacuum ultraviolet (VUV) spectra were recorded from plasmas generated by the NIKE KrF laser for the purpose of observing emission from the two-plasmon decay instability (TPDI) at 2/3 the NIKE wavelength (165 nm). The targets were irradiated by up to 43 overlapping beams with intensity up to $\approx 10^{14}$ W/cm^2 and with beam smoothing by induced spatial incoherence (ISI). The targets consisted of planar foils of CH, BN, Al, Si, S, Ti, Pd, and Au. Titanium-doped silica aerogels in pyrex cylinders were also irradiated. Spectra of the target elements were observed from charge states ranging from the neutral atoms to 5 times ionized. The spectrometer was absolutely calibrated using synchrotron radiation, and absolute VUV plasma emission intensities were determined. Emission from the TPDI at 165 nm wavelength was not observed from any of the irradiated targets. An upper bound on the possible TPDI emission was less than 4×10^{-8} the incident NIKE laser energy. The NIKE laser radiation backscattered from the silica aerogel targets at 248 nm was typically 6×10^{-6} the incident NIKE laser energy, and the spectral broadening corresponded to the 1 THz bandwidth of the ISI smoothing. The spectra from the moderately charged plasma ions (up to 5 times ionized), spectral line widths, absolute continuum emission level, and slope of the continuum were consistent with plasma temperatures in the 100 eV to 300 eV range.

23 February 2005; revised 25 March 2005. Physics of Plasmas.

I. INTRODUCTION

High resolution spectra in the vacuum ultraviolet (VUV) region, generated by intense laser irradiation, are of interest for the spectral diagnostics of the laser-plasma heating mechanism and possible plasma instabilities. For example, the two-plasmon decay instability (TPDI), resulting from the resonant decay of laser energy in the quarter-critical density region, can adversely affect the hydrodynamics of laser fusion targets by localized heating of the lower-density coronal plasma and by heating denser plasma regions by energetic electrons.[1,2] The spectral signature of the TPDI is emission at 2/3 the laser wavelength (frequency $3\omega/2$ where ω is the laser frequency). In practical units, the laser intensity threshold for the TPDI is $I_{14}=AT_{keV}/L_{\mu}\lambda_{\mu}$ where I_{14} is the intensity threshold in units of 10^{14} W/cm^2, T_{keV} is the electron temperature in keV, L_{μ} is the electron density scale length at quarter-critical density in μm, λ_{μ} is the laser wavelength in μm, and A is a numerical factor in the 61.3 to 81.9 range.[2] The intensity threshold increases with decreasing density scale length and laser wavelength. Thus the instability is expected to be suppressed in long scale length plasmas irradiated by shorter laser wavelengths. In addition, it is beneficial to utilize techniques that prevent localized regions of high irradiation intensity that might exceed the instability threshold such as laser beam smoothing and numerous overlapping beams.

Studies of the $3\omega/2$ emission from the TPDI, and the emissions from other laser-plasma interaction instabilities, were carried out using the Lawrence Livermore National Laboratory SHIVA laser.[3] Planar CH foils were irradiated by 1.064 μm laser light focused to $2.5\text{x}10^{15}$ W/cm^2 intensity. When observing at an angle of 60^{o} to the incident laser beams, it was found that 0.04% of the incident laser energy appeared as $3\omega/2$ emission, and 40 keV x-ray emission was

also observed. This and other work stimulated interest in the development of powerful lasers operating at shorter wavelengths and with beam smoothing.

Intensity smoothing by broad bandwidth induced spatial incoherence (ISI) was proposed and implemented at the Naval Research Laboratory (NRL).[4,5] Studies using the NRL frequency-doubled (0.527 μm) Nd-glass PHAROS laser without ISI and with ISI of increasing bandwidths were carried out.[6] The focused laser intensity was 7.5×10^{13} W/cm^2, and the $3\omega/2$ emission was observed at angles of 130^o, 150^o, and 180^o to the normal to the planar targets. It was found that increasing the ISI bandwidth greatly suppressed the $3\omega/2$ and hard x-ray emissions.

Experiments were performed using the 24-beam OMEGA laser with distributed phase plates on all beams and with smoothing by spectral dispersion (SSD).[7] A long scale length plasma was preformed by eight frequency-tripled (0.351 μm) beams focused to 5×10^{13} W/cm^2 intensity, and the plasma was then irradiated by a time-delayed interaction beam (also 0.351 μm) with up to 10^{15} W/cm^2 intensity. When observing the $3\omega/2$ emission at 20^o to the interaction beam, it was found that SSD increased the intensity threshold for $3\omega/2$ emission by a factor of two.

Recent laser-plasma interaction experiments were carried out using the 60-beam OMEGA laser.[8] Spherical gas-filled CH shells were irradiated by 60 beams with 0.351 μm wavelength and two-dimensional SSD. The intensity of the overlapping beams was in the range 6.0×10^{14} to 8.5×10^{14} W/cm^2. The $3\omega/2$ emission, as well as hard x-rays, were observed in all experiments and increased with the overlapping-beam laser intensity.

In this paper, we report the search for the $3\omega/2$ TPDI emission from plasmas created by the NRL NIKE KrF laser with ISI beam smoothing. The laser wavelength was 248 nm, and the intensity of the focused, overlapping NIKE beams was up to $\approx 10^{14}$ W/cm^2. Planar foil targets

consisting of CH, BN, Al, Si, S, Ti, Pd, and Au were irradiated. Titanium-doped silica aerogels in pyrex cylinders were also irradiated. High-resolution spectra in the 150 nm to 250 nm wavelength range were recorded. No evidence of the $3\omega/2$ emission from the TPDI was observed during these experiments. Based on the absolute calibration of the spectrometer using synchrotron radiation, the upper bound on the possible $3\omega/2$ emission was less than $4x10^{-8}$ the incident laser energy.

II. SPECTROMETER CALIBRATIONS

The study of possible TPDI emission from NIKE plasmas, occurring at 2/3 the NIKE laser wavelength (165 nm), required the implementation of a VUV spectrometer. Since the TPDI emission feature is known to be composed of two spectral features centered at a wavelength equal to 2/3 the laser wavelength ($\lambda=2\lambda_L/3$ where λ_L is the laser wavelength) and separated by $\lambda/\Delta\lambda\approx200$,[6,7] the spectrometer must have better than 200 resolving power. In order to identify any spectral features observed near 165 nm as resulting from the TPDI, or to exclude such a possibility, it was necessary to have a thorough understanding of the VUV spectra from a variety of target materials and NIKE laser irradiation conditions. It was also desirable to observe the NIKE laser radiation backscattered from the plasma at 248 nm. Because of these considerations, a high resolution VUV spectrometer covering the 150 nm to 250 nm wavelength range was selected for these studies. The spectrometer was a commercial HR2000 spectrometer modified for VUV spectroscopy.[9] Since transmitting optics could attenuate the shorter wavelengths in the 150 nm to 250 nm range, the spectrometer was specified to have only reflecting optics. The spectrometer was fabricated with vacuum compatible adhesives and other components and was vented to allow outgasing during vacuum pumping.

The spectrometer had a crossed Czerny-Turner f/4 optical system with two mirrors and one diffraction grating. The 2400 groove/mm grating was oriented to cover the 150 nm to 250 nm wavelength range. The spectra were recorded on a CCD linear array with 2048 pixels of 14 μm x 200 μm size. When using a 25 μm wide entrance slit, the expected spectral resolution, corresponding to 2.5 pixels, was 0.122 nm (representing a spectral resolving power of 1350 at 165 nm wavelength).

The digitization of the CCD signal was at the 12 bit level (4096 maximum counts). The spectrometer was controlled by a vacuum compatible USB cable that connected to a vacuum feedthrough, and another USB cable extended 10 m from the vacuum feedthrough to a control computer. It was necessary to shield the two USB cables from electromagnetic interference during the NIKE laser shots.

Extensive tests of the spectrometer capabilities, USB cabling, and control computer were carried out in the laboratory prior to fielding the spectrometer in the NIKE target chamber. A typical spectrum recorded from a mercury vapor lamp is shown in Fig. 1(a). The dark (unilluminated) spectrum, with approximately 100 counts, was subtracted from the spectrum, and the residual noise is at the level of a few counts. There is evidence of scattering on the long wavelength side of the intense 184.888 nm Hg I line, most likely from the grating, at a level approximately a factor of 200 lower than the peak line intensity.

For the initial tests, the spectrometer operated in air, and the wavelength scale was calibrated using the air wavelengths of five mercury lines (indicated in Fig. 1) from the National Institutes of Standards and Technology (NIST) database.[10] It was found that a Lorentzian profile provided the best least-squares fit to the observed mercury lines, and as illustrated in Fig. 1(b) the full width at the half maximum (FWHM) of the 184.888 nm Hg I line was 0.148 nm, slightly

larger than the expected 0.122 nm (2.5 pixel) width. Since the width of the Hg I line from the mercury lamp is intrinsically very narrow, the 0.148 nm observed width is representative of the spectrometer's instrumental width. After establishing the wavelength scale, the average deviation of the five Hg wavelengths from the NIST values was 0.05 nm, approximately a third of the instrumental width.

After recording a number of spectra at the NIKE laser facility, the spectrometer sensitivity was absolutely calibrated at the NRL beamline X24C at the National Synchrotron Light Source. The spectrometer slit was illuminated by monochromatic radiation from the beamline's monochromator in the 150 nm to 240 nm wavelength range. The incident radiation beam was approximately 0.5 mm in diameter, while the spectrometer slit was 25 μm wide and 1 mm high. Thus the radiation beam overfilled the slit width and underfilled the slit height. The spectrometer was mounted on an x-y translation stage so the spectrometer's slit could be centered in the beam. The stage also provided rotational (yaw) motion about a vertical axis along the spectrometer slit. Thus the spectrometer could be centered in the radiation beam in x, y, and yaw.

A slit identical to the spectrometer slit was mounted over a calibrated silicon photodiode for the purpose of measuring the incident radiation intensity. The diode slit was mounted above the spectrometer slit and in the same plane. The diode slit could be translated and centered in the radiation beam. Thus the same beam intensity that passed through the spectrometer slit also passed through the diode slit. By alternately moving the spectrometer slit and the diode slit into the radiation beam at selected wavelengths, the spectrometer counts were related to the photon flux passing through the diode slit at each selected wavelength.

The silicon photodiode was type AXUV100G from International Radiation Detectors Inc.[11] The diode had 10 mm x 10 mm sensitive area. The diode current was measured by a precision electrometer and was converted to absolute photon flux using a previous synchrotron calibration.[12]

When illuminating the spectrometer slit with monochromatic synchrotron radiation at a number of discrete wavelengths in the 150 nm to 240 nm range, it was found that the spectral lines were Lorentzian in shape. For 190 nm incident radiation, the FWHM of the Lorentzian line profile was 0.143 nm and was practically the same as the 0.148 nm width of the 184.888 nm Hg I spectral line shown in Fig. 1(b), which is representative of the spectrometer's instrumental width. This implies that the beam from the monochromator has a spread in wavelength that is smaller than 0.143 nm, and the corresponding monochromator resolving power is larger than 1330. Thus the beamline monochromator has resolving power that is larger than the spectrometer's resolving power (1250 at 184.888 nm wavelength).

The FWHM values derived from the Lorentzian fits to the monochromatic synchrotron radiation spectra are shown in Fig. 2(a). The FWM values decrease from 0.160 nm at 160 nm wavelength to 0.128 nm at 240 nm. Thus the spectrometer's resolving power increases from 1000 at 160 nm to 1880 at 240 nm.

The spectrometer counts were related to the reference diode signal in the following manner. The photons/sec passing through the slit to the reference diode is equal to $i/\rho E$ where i is the diode current, ρ is the diode responsivity in units of A/W (current from the diode divided by the incident radiation power),[12] and E is the photon energy. Thus the photons/sec passing through the diode slit is determined from the diode current, and the same photon flux passes through the spectrometer slit and is recorded as counts. For example, at 190 nm wavelength, the diode

current (4.55 pA after removing the diode's 0.03 pA dark current) measured by a precision electrometer indicated that 4.49×10^7 photons/sec passed through the slit. This photon flux produced 603 counts during a 100 msec spectrometer integration time. Thus the calibration at 190 nm wavelength is 0.000134 counts/photon (7460 photons/count).

The spectrometer calibration curve, in units of counts per incident photon, over the 150-240 nm wavelength range is shown in Fig. 2(b). The error bars represent the square root deviations of the counts in the individual pixels. A straight line was fitted to the log(counts/photon) data points by the least squares technique. The data indicate that the spectrometer's sensitivity decreases exponentially with decreasing wavelength. This is probably related to decreases in the mirror reflectance, grating efficiency, and detector quantum efficiency with decreasing wavelength.

The NIKE spectra were recorded with a protective window between the target and the spectrometer slit, and the transmittances of representative windows were measured using synchrotron radiation. The window was either VUV grade cultured quartz or CaF_2. It was found that the CaF_2 windows significantly degraded during several laser shots, having a pitted and visually translucent appearance. Visual inspection of the cultured quartz windows indicated no noticeable damage during a large number of laser shots. Most of the NIKE spectra were recorded with a cultured quartz window.

In addition to the protective window, for some early laser shots, a pair of crossed cylindrical CaF_2 lenses was positioned behind the protective window and focused a line image of the target emission onto the spectrometer slit. The purpose of the lenses was to increase the flux on the slit and to limit the field of view to the target plasma, excluding surrounding materials that may be indirectly heated by the plasma and scattered laser radiation. The spectrometer and lens

assembly could be precisely translated under computer control in the direction toward the source and laterally in the direction perpendicular to the slit. By using a mercury lamp at the source position, the line image formed by the lenses was positioned on the slit by maximizing the spectrometer counts in the 184.888 nm Hg I line. This was done during the laboratory testing and also in the NIKE target chamber (at air) prior to the laser shots.

The transmittances of representative cultured quartz and CaF_2 windows were measured using monochromatic synchrotron radiation in the 120-240 nm wavelength range as shown in Fig. 3. The windows were mounted on a linear feedthrough and could be moved into the radiation beam provided by the monochromator. The beam transmitted by each window was measured by a reference AXUV100G photodiode (with 10 mm x 10 mm sensitive area) and was normalized by the beam directly incident on the diode when the window was removed from the beam. The transmittances of a CaF_2 window and new and used (to record NIKE spectra) cultured quartz windows are shown in Fig. 3. The comparison of the new and used cultured quartz windows illustrates the decrease in transmittance caused by exposure during the NIKE laser shots.

III. NIKE SPECTRA

The spectrometer was utilized to carry out for the first time a detailed study of high-resolution VUV spectra generated by NIKE laser irradiation. The search for possible TPDI emission near 165 nm wavelength required the analysis of spectra from a variety of targets and NIKE laser irradiation conditions.

The schematic of the experimental layout is shown in Fig. 4. In the initial experiments, the targets were irradiated by overlapping NIKE laser main beams, the planar foil targets were perpendicular to the main beams, and the spectrometer view at an angle of 30^o to the incident

laser beams (spectrometer position 1 in Fig. 4). In subsequent experiments, the targets were irradiated by overlapping NIKE backlighter beams, the planar targets were perpendicular to the laser beams, the spectrometer viewed at an angle of 5^{o} to the incident laser beams (spectrometer position 2 in Fig. 4). In the case of silica aerogel targets, where the aerogels were inside pyrex cylinders, the targets were oriented so the laser beams were incident along the axis of the cylinder.

The spectrometer calibration curve and the window and lens transmittances were used to convert the NIKE spectra from counts/pixel to photons/pixel. This is illustrated in Fig. 5 by a typical spectrum from a silica aerogel target. The target consisted of a pyrex cylinder with 1 mm length and diameter and filled with 3 mg/cm^3 silica aerogel (SiO_2) with 3% titanium doping. The target was irradiated by 5 overlapping NIKE main beams focused to a diameter of 940 μm on the axis of the cylinder. Each beam had 4 ns duration and 43 J energy, and the focused intensity was $8x10^{12}$ W/cm^2. Identified in Fig. 5 are spectral lines from the elements C, B, Al, and Si. According to the manufacturer, the pyrex cylinder had by weight 54% O, 38% Si, 4% boron, 3% Na, and 1% Al. Although the silica aerogel and pyrex targets had no carbon according to the manufacturer, intense carbon lines were observed from these targets and all other NIKE targets except for BN targets that were specially prepared from pure BN stock. The carbon in the silica aerogel spectra may have been adventitious, resulting from contamination during target preparation and handling, or may have been emitted from the target's plastic support.

The spectrometer's wavelength scale was slightly adjusted from the wavelength scale established during the laboratory tests at air. By comparing the wavelengths of a large number of lines in the NIKE spectra with the vacuum wavelengths from the NIST database,[10] the spectrometer's wavelength scale was shifted by +0.02 nm.

The isolated spectral lines from the NIKE plasmas were observed to have Lorentzian profiles with FWHM values in the 0.2 nm to 0.3 nm range, larger than the spectrometer's instrumental width (0.148 nm at 184.888 nm wavelength). The spectral line width exceeding the instrumental width is attributed to Doppler broadening. As shown below, the plasma temperatures are typically in the 100 eV to 300 eV range, and this results in Doppler broadening in the 0.05 nm to 0.09 nm range depending on the ion mass and the wavelength. The spectral line profile resulting from purely Doppler broadening from a Maxwellian velocity distribution would be Gaussian and would be convolved with the broader Lorentzian instrumental profile. Since the broader Lorentzian instrumental profile dominates, the line profiles observed in the NIKE spectra were well fitted by Lorentzian profiles.

The backscattered 248 nm NIKE laser radiation appeared in all spectra and was saturated (>4096 counts) in the spectra from solid targets irradiated by high-energy NIKE laser pulses. However, the backscattered 248 nm radiation was unsaturated in the low-density silica aerogel spectra as shown in Fig. 5. It was found that the NIKE feature was significantly broader than the nearby plasma emission lines, and this was interpreted as a manifestation of the spectral broadening of the NIKE laser irradiation that was smoothed by ISI. Shown in Fig. 6 are Lorentzian fits to the 248 nm NIKE feature and to the nearby 229.76 nm C III line. The FWHM values are 0.353 nm for the NIKE feature and 0.245 nm for the C III line. After removing 0.245 nm broadening from the NIKE feature, the residual width corresponds to 1.2 THz spectral broadening. This is in agreement with the expected NIKE laser bandwidth (≈1 THz) when smoothed by ISI. In addition, the Lorentzian profile of the broadened NIKE feature indicates a coherence time <1 ps which is consistent with the expected 0.7 ps NIKE laser coherence time.

The wavelength of the backscattered NIKE laser radiation shown in Fig. 6(a) is 248.55 nm. Thus the search for emission from the TPDI at 2/3 the NIKE wavelength focused on the 165.70 nm wavelength region. Owing to the intense C I line at 165.7008 nm,[10] as seen in Fig. 5, a search was conducted for other targets materials that have no adventitious carbon and have no other emission lines near 165.70 nm. It was found that boron and nitrogen have no spectral lines near 165.70 nm,[10] and BN targets were prepared by slicing thin wafers from a pure BN rod and polishing the wafers to approximately 25 μm thickness.

Shown in Fig. 7 is the spectrum recorded from a BN target irradiated by 4 overlapping NIKE backlighter beams with 170 J energy and focused to 500 μm diameter and with intensity of $2x10^{13}$ W/cm^2. While the B and N lines are more intense than the C lines, it is apparent in Fig. 7(b) that the 165.7008 nm C I line, and the equally intense 193.0905 nm C I line, are present in the spectrum. Thus any TPDI emission that may be present in the spectrum near 165.70 nm must be at a lower level than the faint 165.7008 nm C I line.

The intensities of the C I lines and other lines from neutral atoms can be reduced by increasing the focused laser intensity and thereby increasing the plasma temperature. This is illustrated in Fig. 8 which shows the spectrum from a BN target irradiated by 43 overlapping NIKE main beams focused to $7x10^{13}$ W/cm^2 intensity. Absent or very weak in the Fig. 8 spectrum are the two C I lines as well as the B I line at 209.023 nm. Figure 8(b) indicates a complete absence of the 165.70 nm TPDI emission.

By using the spectrometer's absolute calibration, the spectra resulting from blackbody emission with assumed temperatures can be compared to the NIKE spectra. Shown in Fig. 9(a) is the spectrum from a BN target irradiated by 4 backlighter beams, the same spectrum as Fig. 7(a), and superimposed blackbody spectra of temperatures 100 eV, 200 eV, and 300 eV. The time-

integrated blackbody spectra were calculated assuming that the plasma emitted for a 10 nsec period and had expanded to a 3 mm source size. Although the continuum in the NIKE spectrum may not be entirely blackbody emission, the continuum intensity level and the slope of the continuum are consistent with temperatures in the 100 eV to 200 eV range. In addition, the ionization indicated by the spectral lines, with charge states up to C IV and N IV, are consistent with temperatures in the 100 eV to 200 eV range. As mentioned above, the spectral line widths observed in the NIKE spectra exceed the instrumental broadening, and the additional broadening is consistent with Doppler broadening resulting from temperatures in the 100 eV to 200 eV range.

Shown in Fig. 9(b) are the blackbody emission curves compared to the spectrum from a 25 μm thick gold foil irradiated by 10 NIKE main beams. The gold spectrum's background level has a higher slope compared to the spectrum from the BN foil shown in Fig. 9(a), and this indicates a higher temperature in the 200-300 eV range. In contrast to the rather simple spectra from the light elements (e.g. CH and BN targets), the spectra from heavier elements such as gold were quite complex. While several spectral lines can be identified as transitions in Au I and other low charge states using the NIST database,[10] the NIST database does not include transitions from charge states higher than Au III, and most spectral lines and broad unresolved features in the gold spectra have not been identified. The complete analysis of the gold VUV spectra produced by the NIKE laser will require further spectroscopic analysis and wavelength calculations.

The highest ionization, up to 5 times ionized C VI, was identified in the spectra from 25 μm thick CH foils with thin metal coatings. Shown in Fig. 10 is the spectrum from a CH foil with a 20 nm thick gold coating that was irradiated by 10 NIKE main beams with 2×10^{13} W/cm^2 focused intensity. Identified in Fig. 10 are the blended C VI n=5-6 transitions at 207.1 nm and

the two C V 1s2s $^3S_1$ – 1s2p ^3P_J transitions with J=2 and J=1 at 227.16 nm and 227.86 nm, respectively. The appearance of transitions in highly charged carbon ions in the spectra from the gold-coated CH target, as well as the numerous lines in the gold foil spectra from high charge states, indicate enhanced coupling of the NIKE laser energy to these gold targets.

IV. TWO-PLASMON DECAY INSTABILITY EMISSION LEVEL

The emission from the TPDI, at 2/3 the NIKE wavelength (165.70 nm), was not observed in any of the numerous spectra recorded from a variety of targets and NIKE laser conditions. An upper bound on the possible 165.70 nm emission from the TPDI can be determined from the spectrometer calibration. For example, in the spectra recorded when the spectrometer slit was 38 cm from targets irradiated by 43 NIKE main beams and using a cultured quartz window and no lenses, the total counts above the background continuum level near 165.70 nm were less than 100. Thus the number of photons producing these counts was less than 1.8×10^6. Considering the area of the spectrometer slit (25 μm x 1 mm), the 38 cm standoff distance, and the transmittance of the cultured quartz window, the plasma emission near 165.70 nm was less than 0.08 mJ assuming isotropic emission into 2π solid angle. For the case of 43 NIKE main beams, each with 43 J energy, the conversion factor from NIKE energy to 165.70 nm emission was less than 4×10^{-8}.

The absence of detectable TPDI emission from plasmas created by overlapping NIKE laser beams smoothed by ISI is consistent with the predicted intensity threshold. As discussed in Section I, the laser intensity threshold for the TPDI is $I_{14}=AT_{keV}/L_\mu\lambda_\mu$ in practical units. For the typical NIKE laser conditions, the parameter A is equal to 81, and hydrodynamic modeling indicates the density scale length at quarter-critical density is L_μ=120 μm. Using T_{keV}=0.3 keV, the TPDI intensity threshold is 8×10^{13} W/cm^2. The average focused NIKE intensity was

comparable to or smaller than this value, and beam smoothing and overlapping of the beams prevented localized hot spots that exceeded the TPDI intensity threshold.

The fraction of the incident NIKE laser energy that was backscattered from the target (at the 248.55 nm NIKE wavelength) was determined from the spectra recorded from the low-density silica aerogel targets, where the NIKE feature was not saturated in the spectra. For example, in the spectrum shown in Figs. 5 and 6, the spectrometer calibration indicates that 1.2 mJ of 248.55 nm NIKE laser irradiation was backscattered (assuming isotropic scattering into 2π solid angle). The target was irradiated by 5 NIKE main beams, and the fraction of incident laser energy that was backscattered was 6×10^{-6}. The scattered fraction is expected to be much higher from dense plasmas from solid targets, and this resulted in saturation of the NIKE feature in those spectra. The scattered fraction is an important consideration for implementation of a Thomson scattering diagnostic, for example using an Nd-glass frequency-quadrupled laser at 266.0 nm wavelength.

V. CONCLUSIONS

Numerous VUV spectra from a variety of targets and NIKE laser conditions were analyzed, and TPDI emission at 2/3 the NIKE wavelength was not observed in any of the spectra. Up to 43 overlapping NIKE beams with ISI smoothing and up to $\approx 10^{14}$ W/cm^2 focused intensity were utilized. Based on the absolute calibration of the spectrometer, the upper bound on the possible TPDI emission was less than 4×10^{-8} the incident NIKE laser energy. By comparison, the fraction of incident NIKE laser energy backscattered from low-density silica aerogel targets was 6×10^{-6}. The NIKE feature has a Lorentzian shape and width consistent with the NIKE laser 1 THz bandwidth and 0.7 ps coherence time resulting from ISI smoothing.

Further studies are planned using a custom designed VUV imaging spectrometer with much higher sensitivity and spatial resolution and with time resolution. The spectrometer consists of a Cassegrain telescope and a high resolution two-grating spectrometer with excellent imaging properties that are optimized for 165 nm diffraction in the direction normal to the gratings (Wadsworth grating mount). The spatially resolved, time integrated spectral images will be recorded on a two-dimensional CMOS detector. The time resolved spectra will be recorded by an absolutely calibrated silicon photodiode linear array as utilized in the extreme ultraviolet region in NIKE transmission grating spectrometers.[13] Sub-nanosecond time resolution and high spatial resolution will greatly enhance the ability to distinguish between the 165.70 nm TPDI emission, occurring in the focal spot during the high-intensity laser pulse, from the spectral line and continuum emission outside the focal spot and following the laser pulse, particularly the 165.7008 nm C I line. The increased sensitivity of the new VUV spectrometer will allow the observation of possible TPDI emission from NIKE plasmas at a level that is 270 below the level possible in the present study, a factor of 1.5×10^{-10} times the incident NIKE laser energy. This will further quantify the capability of overlapping NIKE laser beams with ISI smoothing to suppress the two-plasmon decay instability.

Acknowledgements

We thank the NIKE laser operations staff and target chamber staff for invaluable assistance. This work was supported by the U. S. Department of Energy. The mention of commercial products does not necessarily represent an endorsement.

References

1. C. S. Liu and M. N. Rosenbluth, Phys. Fluids **19**, 967 (1976).
2. A. Simon, R. W. Short, E. A. Williams, and T. Dewandre, Phys. Fluids **26**, 3107 (1983).
3. D. W. Phillion, E. M. Campbell, K. G. Esterbrook, G. E. Phillips, and F. Ze, Phys. Rev. Lett. **49**, 1405 (1982).
4. R. H. Lehmberg and S. P. Obenschain, Opt. Commun. **46**, 27 (1983).
5. R. H. Lehmberg, A. J. Schmitt, and S. E. Bodner, J. Appl. Phys. **62**, 2680 (1987).
6. T. A. Peyser, C. K. Manka, S. P. Obenschain, and K. J. Kearney, Phys. Fluids B **3**, 1479 (1991).
7. W. Seka, R. E. Bahr, R. W. Short, A. Simon, and R. S. Craxton, Phys. Fluids B **4**, 2232 (1992).
8. C. Stoeckl, R. E. Bahr, B. Yaakobi, W. Seka, S. P. Regan, R. S. Craxton, J. A. Delettrez, R. W. Short, J. Myatt, A. V. Maximov, and H. Baldis, Laboratory for Laser Energetics Review, vol. 94, 76 (2003).
9. Ocean Optics Inc., 830 Douglas Ave., Dunedin FL 34698.
10. Atomic Spectra Database, National Institutes of Standards and Technology, http://physics.nist.gov/cgi-bin/AtData/main_asd.
11. International Radiation Detectors Inc., 2527 West 237th Street Unit A, Torrance, CA 90505.
12. M. Richter, U. Kroth, A. Gottwald, C. Gerth, K. Tiedtke, T. Saito, I. Tassy, and K. Volger, Appl. Opt. **41**, 7167 (2002).
13. J. L. Weaver, U. Feldman, J. F. Seely, G. Holland, V. Serlin, M. Klapisch, D. Columbant, and A. Mostovych, Phys. of Plasmas, **8**, 5230 (2001).

Figure Captions

FIG. 1. (a) Laboratory spectrum from a mercury vapor lamp. (b) Fit of a Lorentzian profile to the Hg I 184.888 nm spectral line.

FIG. 2. (a) Linewidths measured using synchrotron radiation (square data symbols) and using the mercury vapor lamp (triangular symbol). (b) Spectrometer calibration curve in units of counts per incident photon.

FIG. 3. Transmittances of new (unused) and used cultured quartz windows and a new CaF_2 window measured using synchrotron radiation.

FIG. 4. Schematic of the incident laser beams, target orientation, and spectrometer position: position 1 for main beam irradiation of the target (solid line), and position 2 for backlighter beam irradiation of the target (dashed line).

FIG. 5. Spectrum recorded from a laser-irradiated silica aerogel in a pyrex cylinder in units of (a) counts per pixel and (b) photons per pixel.

FIG. 6. Fits of Lorentzian profiles to (a) the 248.55 nm NIKE laser backscattered feature and (b) the 229.76 nm C III spectral line.

FIG. 7. (a) Spectrum from a BN target irradiated by 4 NIKE laser backlighter beams and (b) details of the spectrum in the 160 nm to 200 nm range.

FIG. 8. Spectrum from a BN target irradiated by 43 NIKE laser main beams and (b) details of the spectrum in the 160 nm to 170 nm range.

FIG. 9. Comparison of the calculated emission from blackbody plasmas with temperatures of 100 eV, 200 eV, and 300 eV with spectra from (a) a BN foil irradiated by 4 NIKE laser backlighter beams and (b) a 25 μm thick gold foil target irradiated by 10 main NIKE beams.

FIG. 10. (a) Spectrum from a 25 μm thick CH foil with a 20 nm gold coating and irradiated by 10 main NIKE beams and (b) spectral lines from highly charged carbon ions.

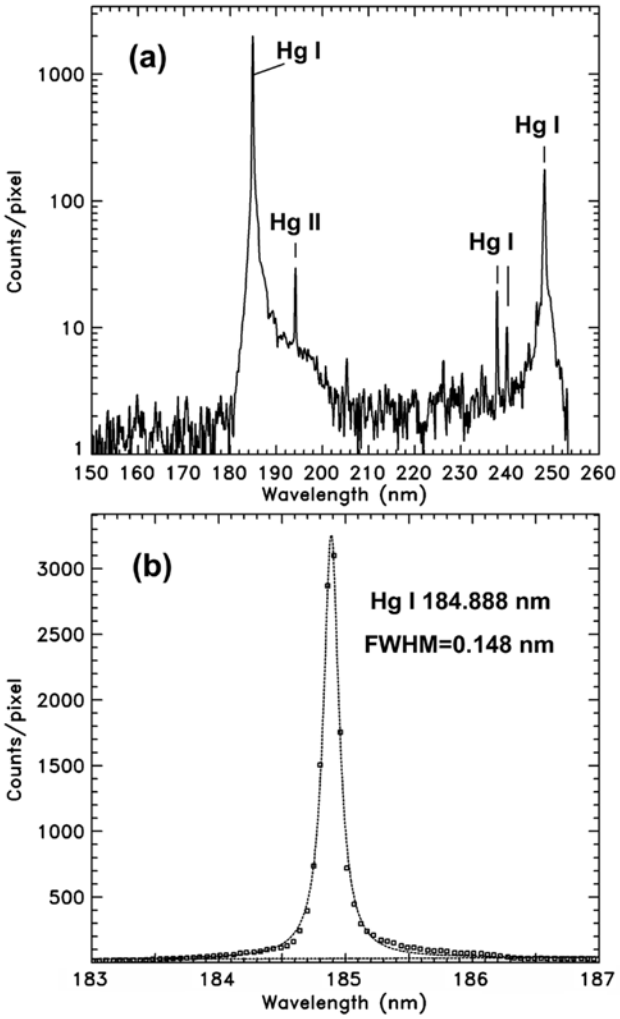
(a)
Hg I
Hg II
Hg I
Hg I
Counts/pixel
1000
100
10
1
150 160 170 180 190 200 210 220 230 240 250 260
Wavelength (nm)
(b)
Hg I 184.888 nm
FWHM=0.148 nm
Counts/pixel
3000
2500
2000
1500
1000
500
183 184 185 186 187
Wavelength (nm)

Figure 1

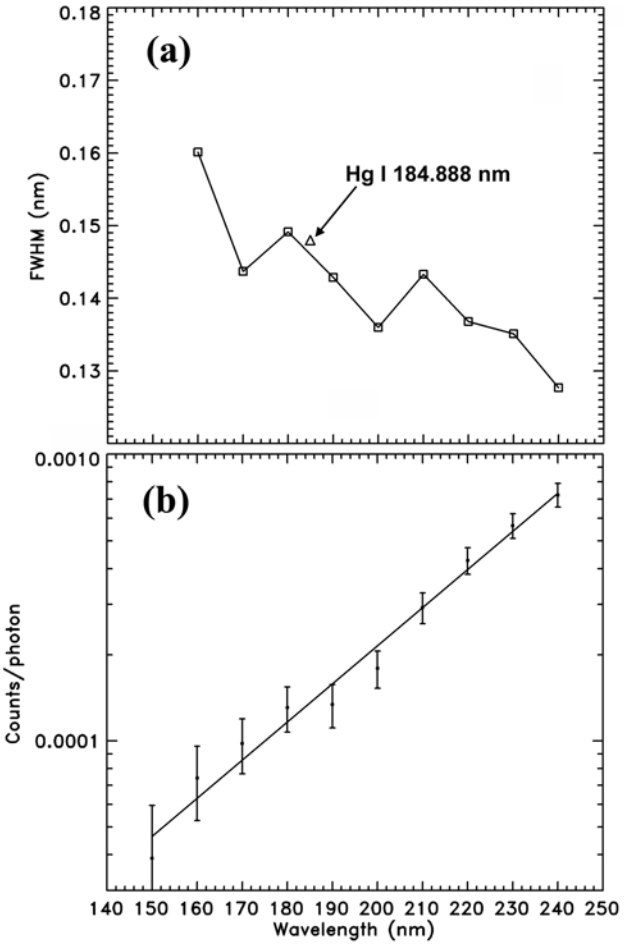
(a)
Hg I 184.888 nm
FWHM (nm)
0.18
0.17
0.16
0.15
0.14
0.13
(b)
Counts/photon
0.0010
0.0001
140 150 160 170 180 190 200 210 220 230 240 250
Wavelength (nm)

Figure 2

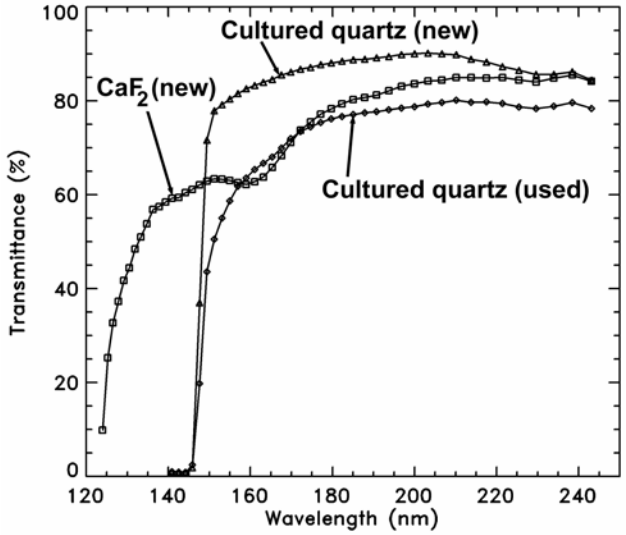
Cultured quartz (new)
CaF2 (new)
Cultured quartz (used)
Transmittance (%)
Wavelength (nm)
100
80
60
40
20
0
120
140
160
180
200
220
240

Figure 3

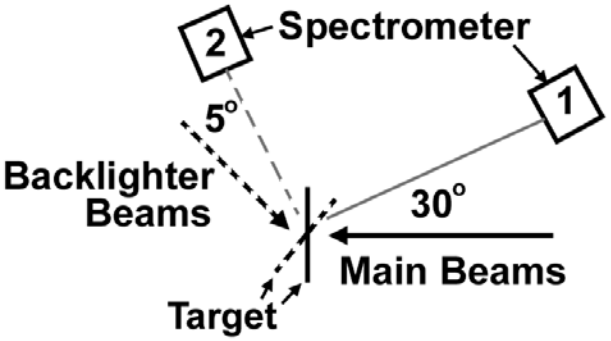

Figure 4

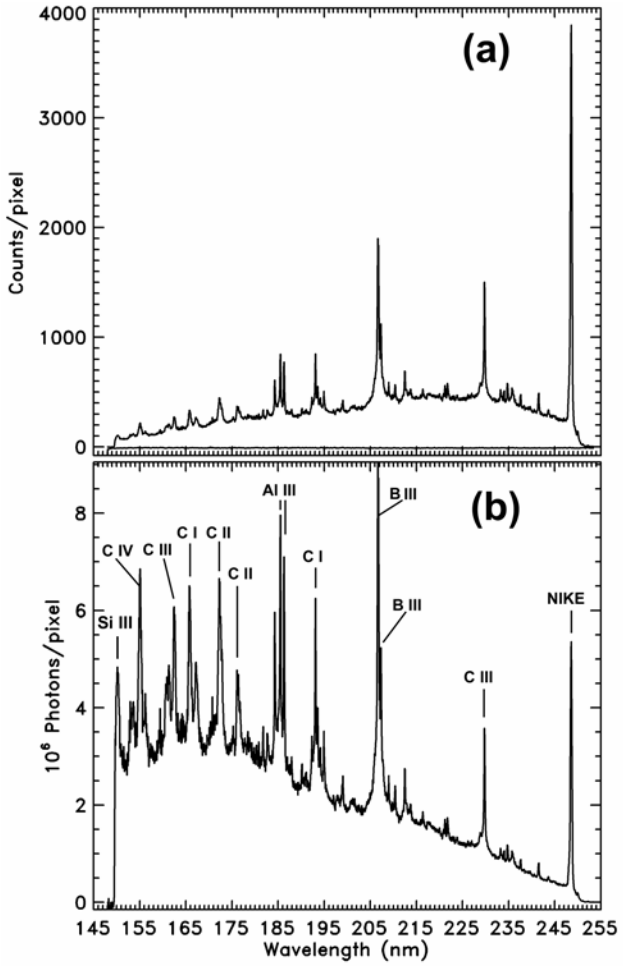
(a)
(b)
Counts/pixel
10^6 Photons/pixel
Wavelength (nm)
Si III
C IV
C III
C I
C II
C II
Al III
C I
B III
B III
C III
NIKE

Figure 5

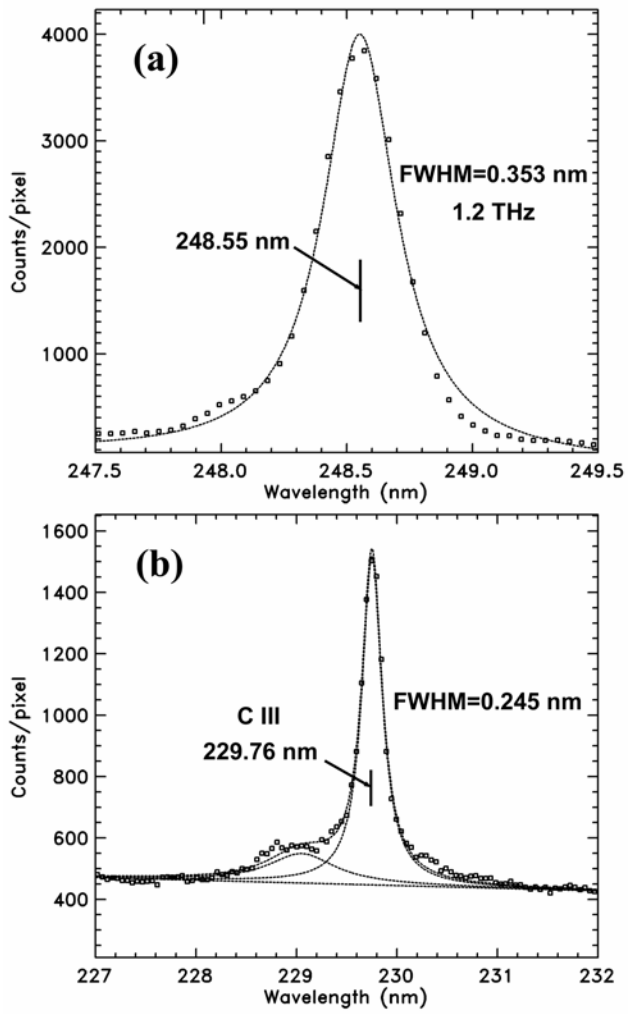
(a)
FWHM=0.353 nm
1.2 THz
248.55 nm
Counts/pixel
Wavelength (nm)
(b)
C III
229.76 nm
FWHM=0.245 nm
Counts/pixel
Wavelength (nm)

Figure 6

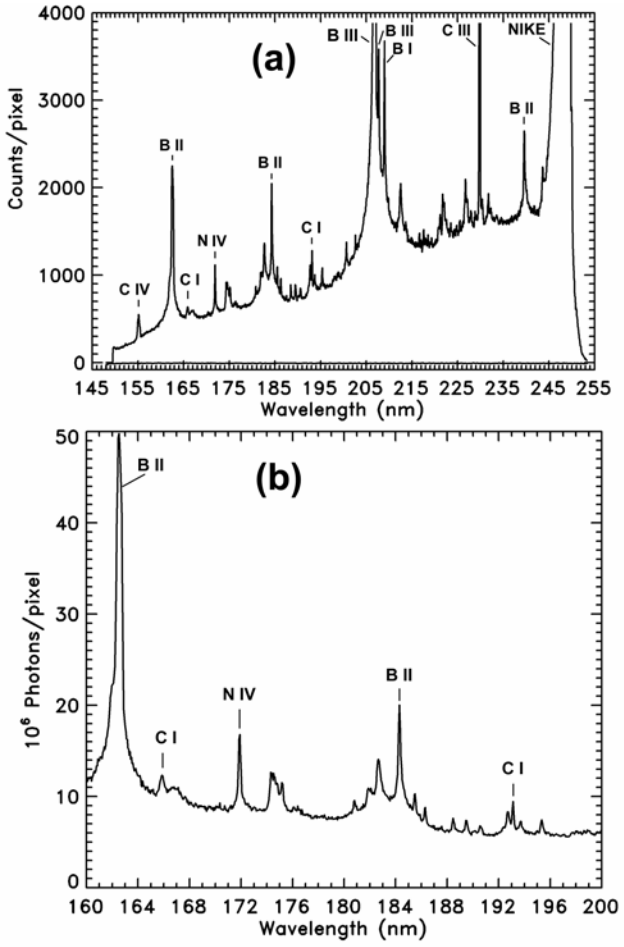
(a)
Counts/pixel
Wavelength (nm)
B III
B III
B I
C III
NIKE
B II
B II
B II
C IV
C I
N IV
C I
(b)
10^6 Photons/pixel
Wavelength (nm)
B II
C I
N IV
B II
C I

Figure 7

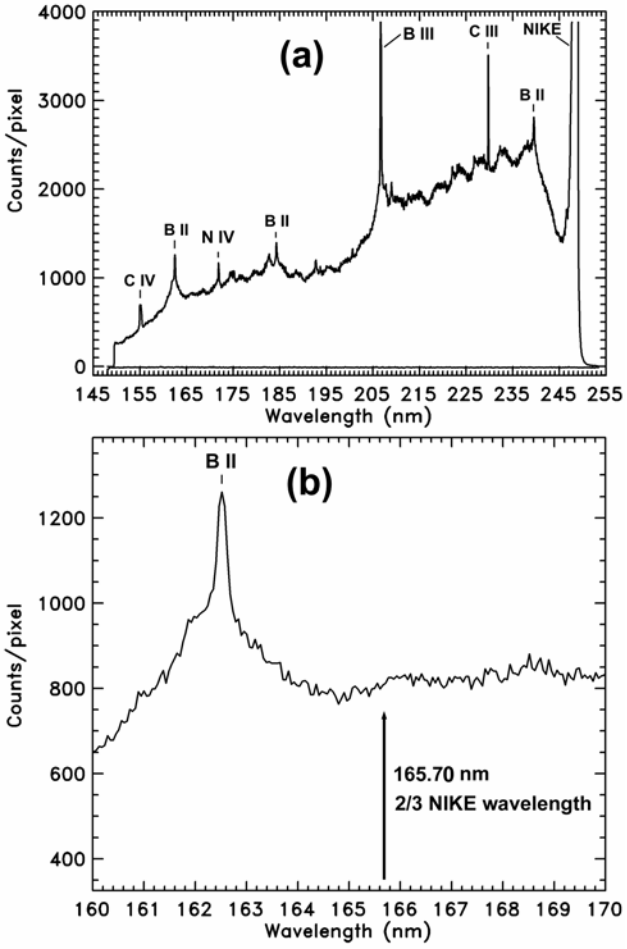
(a)
B III
C III
NIKE
B II
B II
N IV
B II
C IV
Counts/pixel
Wavelength (nm)
(b)
B II
165.70 nm
2/3 NIKE wavelength
Counts/pixel
Wavelength (nm)

Figure 8

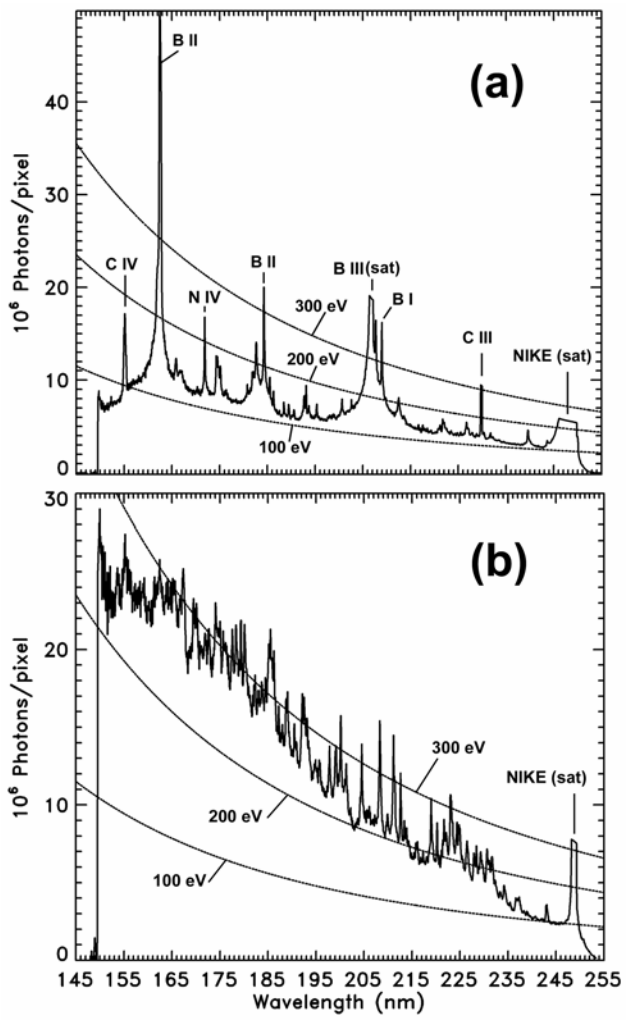
(a)
B II
C IV
N IV
B II
B III(sat)
B I
C III
NIKE (sat)
300 eV
200 eV
100 eV
10⁶ Photons/pixel
(b)
300 eV
NIKE (sat)
200 eV
100 eV
10⁶ Photons/pixel
Wavelength (nm)

Figure 9

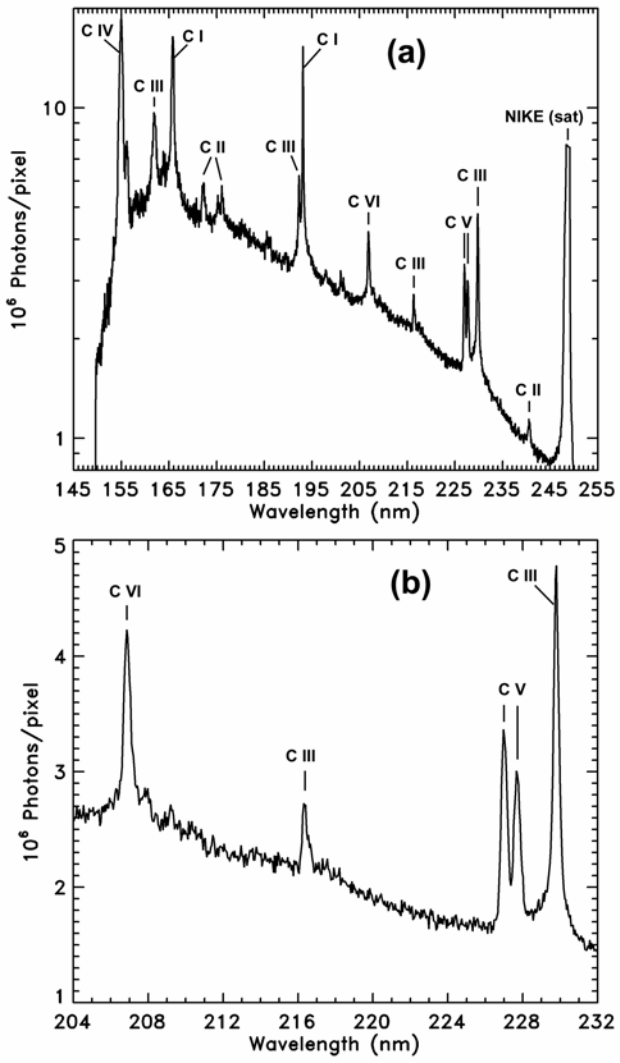
(a)
C IV
C III
C I
C II
C I
C III
C VI
C III
C V
C III
C II
NIKE (sat)
10
1
10^6 Photons/pixel
145 155 165 175 185 195 205 215 225 235 245 255
Wavelength (nm)
(b)
C VI
C III
C V
C III
5
4
3
2
1
10^6 Photons/pixel
204 208 212 216 220 224 228 232
Wavelength (nm)

Figure 10